MACH 6 AEROTHERMOELASTIC EXPERIMENT WITH SHOCK IMPINGEMENT ON A COMPLIANT PANEL UNDER THERMAL AND MECHANICAL BUCKLING

Damon O. Kirkpatrick*, Dylan D. Dooner, Andrew J. Neely, Charles M. Hoke, Timothy J. Beberniss and David R. Buttsworth

The University of New South Wales
1 Northcott Drive, Canberra, ACT, 2612
Australia

ABSTRACT

MAIN RESEARCH QUESTION

Vehicle designers and stakeholders are invested in increasing the service life and survivability of reusable high-speed aircraft. Starting around Mach 3 and certainly when flying at speeds greater than Mach 5, the vehicle can be exposed to large aerodynamic forces, including impinging shocks, and extreme temperatures, primarily due to viscous dissipation [1]. As a principal part of the external structure, skin panels bear cyclic and static aerodynamic, thermal and mechanical loads which can cause the panels to experience fatigue and buckle [2]. While many experiments in the literature have analyzed fluid-thermal-structural interations (FTSI) and shock wave/boundary layer interactions (SBLI) on representative skin panels [2-9], very few [10] have attempted to isolate and quantify the effects of panel buckling on the panel's response. This study consists of wind tunnel experiments conducted to more fully understand the underlying mechanisms of the coupled interactions between aerodynamic, thermal and mechanical loads on a compliant, buckled structure in high-speed flow. This investigation's contributions expand the FTSI and SBLI knowledge base and provide an experimental database that could help validate high-speed simulations and inform vehicle design.

RESEARCH METHOD

A 0.032-inch-thick, Aluminum7075-T6 panel with a planform area of (120x60) mm and clamped-free-clamped-free (CFCF) structural boundary conditions (Figure 1b) was tested under Mach 6 conditions in the free-piston compression Ludwieg tube at the University of Southern Queensland (TUSQ). The facility allows for nominal run durations of approximately 200 milliseconds at the Mach 6 condition. A variable-incidence 10° wedge, pictured in Figures 1a and 1c, was mounted above and upstream of the panel and wind tunnel support structure. The angle of incidence of the wedge, or flow deflection angle, θ_f, was fixed at 2° and 10° for the two sets of experiments. The wedge generated an oblique shock that impinged on the panel, and its response was observed. Each panel was tested with four buckling states: non-buckled (NB) at room temperature, 26 ℃ (T_w/T_0= 0.56), mechanically buckled (MB) by applying an axial force at the trailing edge of the panel at room temperature, non-buckled by allowing thermal expansion in the longitudinal direction at 190 ℃ (T_w/T_0= 0.87) and thermally buckled (TB) via restricting longitudinal thermal expansion from 175 ℃ to 190 ℃. Additionally, the downwind structure to which the panel's trailing edge was clamped rested on a dovetail slide. The downwind structure could translate forward to induce the mechanical buckle and backward to allow for thermal expansion, then be secured in place by tightening four M5 screws into the model baseplate. These test cases are summarized in Table 1.

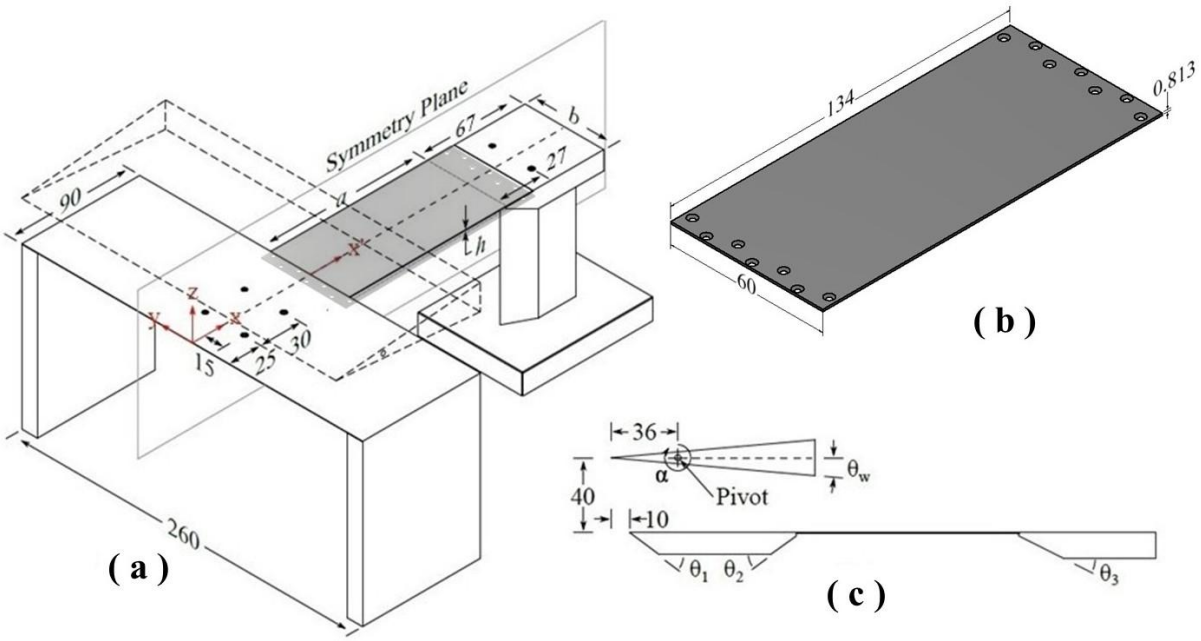

Figure 1: (a) Wind tunnel model support structure and shock generator with (b) test panel and (c) cross-sectional axial centerline view where, $\theta_w = 5°$, $\theta_1 = 36.5°$, $\theta_2 = 35.5°$ and $\theta_3 = 35°$.

Table 1: Test matrix for FTSI and SBLI experiments.

Test Case	**θ_f [°]**	**NB/MB/TB**	**T_w [°C]**	**T_w/T_0 [-]**
1	2	NB	26.5	0.56
2	2	MB	26.0	0.56
3	2	NB	189	0.86
4	2	TB	194	0.87
5	10	NB	25.5	0.56
6	10	MB	25.3	0.56
7	10	NB	191	0.87
8	10	TB	193	0.87

Multiple diagnostics were used to measure panel deflection, visualize the flow, monitor the panel temperature and characterize the panel's natural and aerodynamically forced frequencies. The list of the instrumentation with the derived data from each is outlined in Table 2.

Table 2: Instrumentation used for the present study.

Instrumentation	Quantity	Derived Data
Pressure transducer	4	Local/tunnel barrel pressures
Schlieren camera	1	Flow density gradient images
High-speed monochrome camera	2	Stereoscopic DIC
Laser point displacement sensors	2	Local panel deflection
Laser Doppler vibrometer	1	Panel natural frequencies
High-temperature strain gauge	2	Panel strain at trailing edge
Two-color pyrometer	1	Panel temperature
IR thermal imaging camera	1	Panel temperature distribution

RESULTS

Figures 2 and 3 include preliminary results from a frequency analysis of the displacement time history measured by a Micro-Epsilon ILD1420-200(002) Laser Point Displacement Sensor (PDS) located at (60, 28) mm, relative to the panel-centric axes system from Figure 1a. Effectively, the PDS was measuring the displacement of the right edge of the panel at its longitudinal center. The frequency analysis of the displacement time history at this location on the panel showed the panel's first and second forced frequencies. The first forced frequency was the panel's first bending mode, and the second forced frequency was its first torsional mode. Welch's method with a full Hann window and an NFFT equal to the power of two greater than the signal length was used to estimate the power spectral densities (PSD).

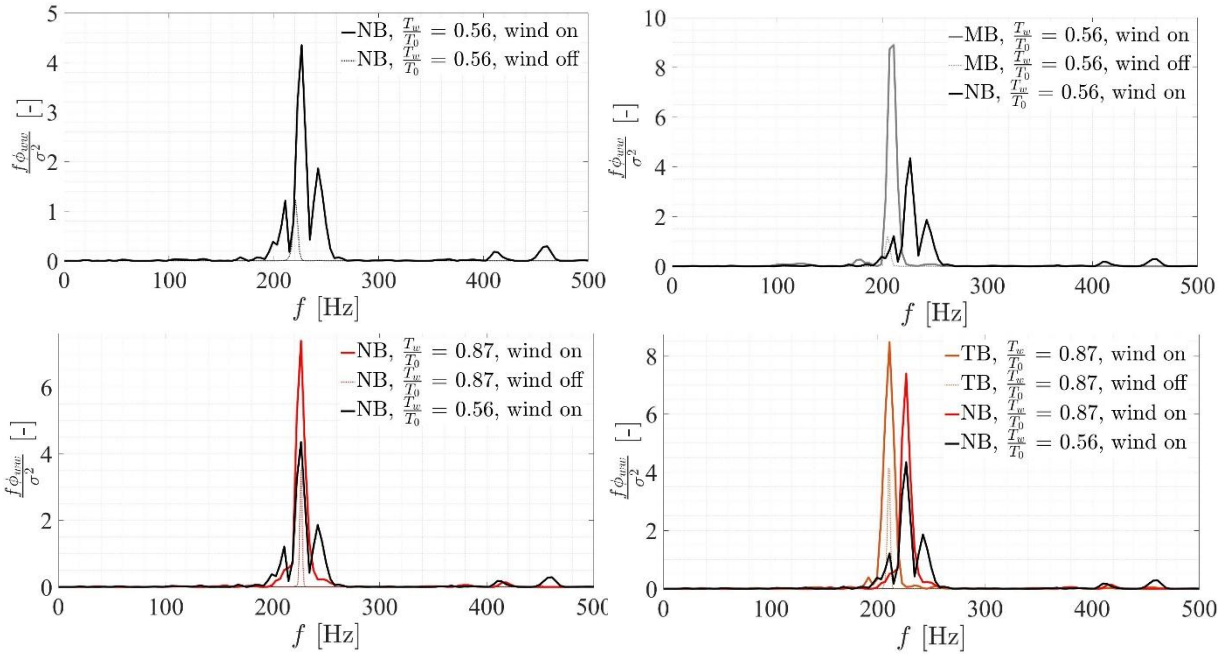

Figure 2: Normalized PSDs for test cases 1-4, with $\theta_f = 2°$ and "wind on" (solid) and "wind off" (dotted) responses separated.

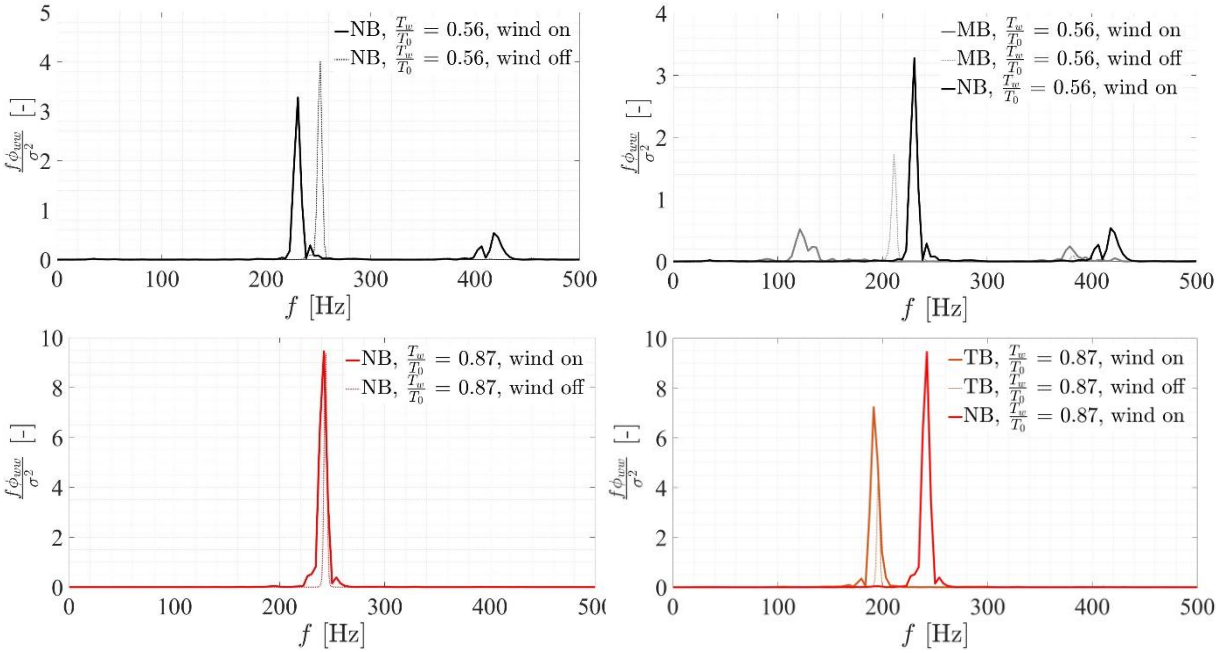

Figure 3: Normalized PSDs for test cases 5-8, with $\theta_f = 10°$ and "wind on" (solid) and "wind off" (dotted) responses separated.

The preliminary results seemed to indicate that the stronger the shock, and consequently the greater the pressure differential above and below the panel, the greater the decrease of the first forced frequency of the buckled panel when compared to the first forced frequency of the same non-buckled panel at the equivalent temperature. Further analysis of additional diagnostics will likely corroborate and help explain these initial findings.

CONCLUSIONS

Eight experimental test cases of a variably buckled, CFCF compliant panel with an impinging shock in Mach 6 flow were analyzed. The panel was mechanically buckled at room temperature (nominally 26 °C) and thermally buckled by preventing thermal expansion in the x-direction as the panel was heated from 175 °C to 190 °C. The results of these buckled test cases were compared to test cases where the panel was not buckled at the same respective temperatures. The stronger shock at $\theta_f = 10°$ tended to exacerbate the reduction in the panel's first aerodynamically forced frequency when the panel was either mechanically or thermally buckled. The understanding of the coupled phenomena inherent in FTSI and SBLI gained from these sets of experiments could be factored into high-speed vehicle design and development.

REFERENCES

[1] John D. Jr. Anderson. Hypersonic and High-Temperature Gas Dynamics. Third. American Institute of Aeronautics & Astronautics, Oct. 2019, pp. 15–30.

[2] Morton, M. (2007, April 23). Certification of the F-22 Advanced Tactical Fighter for High Cycle and Sonic Fatigue. 48th AIAA/ASME/ASCE/AHS/ASC Structures, Structural Dynamics, and Materials Conference. https://doi.org/10.2514/6.2007-1766

[3] Willems, S., Gülhan, A., & Esser, B. (2013). Shock Induced Fluid-Structure Interaction on a Flexible Wall in Supersonic Turbulent Flow. https://doi.org/10.1051/eucass/201305285

[4] Vasconcelos, P. B., McQuellin, L. P., Talluru, K. M., & Neely, A. J. (2023). High-Speed Fluid-Structure Interactions on a Compliant Panel Under Shock Impingement. AIAA Journal, 61(3), 1077–1094. https://doi.org/10.2514/1.J061886

[5] D'Aguanno, A., Quesada Allerhand, P., Schrijer, F. F. J., & van Oudheusden, B. W. (2023). Characterization of Shock-Induced Panel Flutter with Simultaneous Use of DIC and PIV. Experiments in Fluids, 64(1), 15.https://doi.org/10.1007/s00348-022-03551-1

[6] Shi, A., He, Y., & Dowell, E. H. (2024, January 1). A Brief Review of Panel Aeroelasticity with Shock Interaction. ICAS Proceedings.

[7] Varigonda, S. V., & Narayanaswamy, V. (2023). Fluid Structure Interactions Generated by an Oblique Shock Impinging on a Thin Elastic Panel. Journal of Fluids and Structures, 119, 103890. https://doi.org/10.1016/j.jfluidstructs.2023.103890

[8] Acosta, A. R., & Austin, J. M. (2024, January 8). Experimental Investigation of an Impinging Shock-Boundary Layer Interaction on a Compliant Panel in Mach 4 Flow. AIAA SCITECH 2024 Forum. https://doi.org/10.2514/6.2024-1153

[9] Tripathi, A., Gustavsson, J., Shoele, K., & Kumar, R. (2024). Effect of Shock Impingement Location on the Fluid–Structure Interactions over a Compliant Panel. Shock Waves, 34(1), 1–19. https://doi.org/10.1007/s00193-024-01162-9

[10] Brouwer, K. R., Perez, R. A., Riley, Z. B., Beberniss, T. J., and Spottswood, S. M., "Measurements of a thermally buckled panel dynamically excited by a separated shock/boundary-layer interaction," Aerospace Science and Technology, Vol. 168, 2026, p. 111066. https://doi.org/10.1016/j.ast.2025.111066.